nature chemical biology

ARTICLE

PUBLISHED ONLINE: 11 APRIL 2016 | DOI: 10.1038/NCHEMBIO.2064

Optogenetic oligomerization of Rab GTPases regulates intracellular membrane trafficking

Mai Khanh Nguyen[1], Cha Yeon Kim[2], Jin Man Kim[3], Byung Ouk Park[4], Sangkyu Lee[4], Hyerim Park[1] & Won Do Heo[1,4,5]*

Intracellular membrane trafficking, which is involved in diverse cellular processes, is dynamic and difficult to study in a spatiotemporal manner. Here we report an optogenetic strategy, termed light-activated reversible inhibition by assembled trap of intracellular membranes (IM-LARIAT), that uses various Rab GTPases combined with blue-light-induced hetero-interaction between cryptochrome 2 and CIB1. In this system, illumination induces a rapid and reversible intracellular membrane aggregation that disrupts the dynamics and functions of the targeted membrane. We applied IM-LARIAT to specifically perturb several Rab-mediated trafficking processes, including receptor transport, protein sorting and secretion, and signaling initiated from endosomes. We finally used this tool to reveal different functions of local Rab5-mediated and Rab11-mediated membrane trafficking in growth cones and soma of young hippocampal neurons. Our results show that IM-LARIAT is a versatile tool that can be used to dissect spatiotemporal functions of intracellular membranes in diverse systems.

© 2016 Nature America, Inc. All rights reserved.

Intracellular membrane trafficking is a complex conserved process in eukaryotic cells. Trafficking events (e.g., transport, tethering, docking and fusion) mediate and participate in diverse intracellular processes. Recent studies have increased our knowledge of vesicle-trafficking functions, which include ensuring the synthesis and distribution of intracellular proteins and regulating signal transduction[1,2]. An impairment in any trafficking step can alter cell metabolism, cell polarization and/or specific signaling pathways, and may be associated with severe diseases, including cancer, immunodeficiency and neurological disorders[3–5].

Intracellular membranes are highly dynamic in their properties, and few tools are available to specifically modulate the different types of membranes in a spatiotemporally precise fashion. Genetic perturbation (e.g., gene deletion, RNA interference and overexpression of mutant proteins) has been widely used to study intracellular membrane trafficking, but such genetic modifications are slow to exert their effects, and tend to induce side effects and irreversible changes in the structures and properties of membranes[6]. Small-molecule inhibitors and nonpermissive temperatures have also been used as research tools in this context, but those strategies have been limited by poor selectivity and low reversibility[7]. An alternate approach is to change intracellular membrane lipids with a rapamycin-based system, which triggers tubularization of the endosomal compartment and blocks its normal functions[8]. However, this method has been limited by its relatively narrow application range and poor reversibility.

Recently developed optogenetic tools enable powerful approaches for overcoming these limitations and conferring a high degree of spatiotemporal resolution. In this context, many flavoproteins have attracted research attention, including the light-, oxygen- or voltage-sensing (LOV) domain, the blue-light-using flavin (BLUF) protein, and the blue-light-sensing cryptochrome 2 (CRY2) from *Arabidopsis thaliana*. Many groups have recently used CRY2, which, together with its dimerization partner, CIB1, can self-oligomerize to activate/inhibit signaling proteins[9–15]. In the context of trafficking studies, UVR8, a plant ultraviolet receptor protein that forms homodimers in the dark and dissociates to monomers upon UV-B illumination, has been used to trigger local protein secretion at neuronal dendritic branch points[16]. This tool allows the motoring of secretory protein trafficking at a local and acute level, but it may have drawbacks, including limited application in diverse trafficking studies and the toxicity of UV-B light.

Rab GTPases, which constitute the largest subfamily of small GTPases, have over 60 known members in humans, are key actors in membrane physiology, and can mediate diverse trafficking processes[17–19]. Rab GTPases undergo molecular switching between the active GTP-bound form and the inactive GDP-bound form to recruit effectors that regulate trafficking processes. Rab GTPases also contribute to activating signaling molecules (e.g., Rac1 and p110β) via scaffold assembly[2,20,21]. The functional impairments of Rab GTPases have been associated with diseases of vesicle trafficking dysfunction[17,19]. Although we do not yet fully understand the functional mechanisms of all Rab GTPases, they are broadly recognized as markers for specific intracellular membrane organelles[18].

Here we used several Rab GTPases to analyze different intracellular membranes. Given the fast dynamics of trafficking events, we used the N-terminal photolyase homology region (PHR) from CRY2 and a truncated N-terminal sequence from CIB1 (hereafter called CRY2 and CIB1, respectively). CRY2 and CIB1 bind within seconds after illumination with blue light, and dissociate a few minutes thereafter in the dark state (dissociation half-time ($t_{1/2}$) = 5.5 min)[9]. Our results revealed that that the light-induced binding of CRY2 and CIB1 conjugated to Rab GTPases, together with the self-oligomerization of CRY2, rapidly induced the aggregation and functional disturbance of early and recycling endosomes (marked by Rab5 and Rab11, respectively). We applied IM-LARIAT to various Rab-targeted membranes, and report that the induced aggregation can inhibit or delay functions of other trafficking pathways, including the late trafficking pathway, protein transport along the endocytic reticulum (ER)-Golgi-plasma membrane (PM), and the

[1]Department of Biological Sciences, Korea Advanced Institute of Science and Technology (KAIST), Daejeon, Republic of Korea. [2]Graduate School of Nanoscience and Technology, KAIST, Daejeon, Republic of Korea. [3]Graduate School of Medical Science and Engineering, KAIST, Daejeon, Republic of Korea. [4]Center for Cognition and Sociality, Institute for Basic Science (IBS), Daejeon, Republic of Korea. [5]KAIST Institute for the BioCentury, KAIST, Daejeon, Republic of Korea. *e-mail: wondo@kaist.ac.kr

secretory pathway. Finally, we used our new tool on Rab5- and Rab11-targeted membranes in hippocampal neurons, a more complex system that must be analyzed in a spatial and temporal manner, and showed that different populations of Rab5- and Rab11-targeted compartment in growth cones (GCs) or soma have different roles during dendritic growth. These results showed that IM-LARIAT could increase our understanding of the distinct functions of intracellular trafficking processes, especially in complex systems such as neurons.

RESULTS

IM-LARIAT design

To develop a system that would enable high-resolution spatial perturbation of membrane trafficking, we decided to conjugate Rab GTPases directly to the light-sensitive module, CRY2. As an example, we targeted Rab5, which is a well-known Rab GTPase that localizes to membranes of early endosomal compartments. However, CRY2–Rab5 transfected cells demonstrated aberrant membrane structures and slow dynamics even before exposure to light. CIB1–Rab5 transfected cells did not have such aberrant membrane structures (**Supplementary Results**, **Supplementary Fig. 1a–c** and **Supplementary Video 1**), perhaps because CRY2 is consistently dimerized in the dark[22]. To confirm that the conjugation of CIB1 to the N terminus of Rab GTPases allowed the GTPases to retain function on specific membranes, we knocked down endogenous Rab5 and transfected cells with a construct encoding CIB1–Rab5. Cells treated with Rab5 siRNA, as compared to those treated with control siRNA, had decreased vesicle surface expression of EEA1, a typical Rab5 effector, but this was rescued by transfection of CIB1-Rab5 (**Supplementary Figs. 1e**,**f** and **11**), suggesting that CIB1-Rab5 is functionally similar to Rab5. Next, we expressed CIB1–Rab5 or CIB1-Rab11 (Rab GTPases that localize to membranes of endosomal compartment) in cells expressing CRY2, and used blue light to conditionally induce the interaction between CRY2 and CIB1–Rab (**Fig. 1a**). When exposed to blue light, CRY2 simultaneously self-oligomerized and bound to multiple CIB1–Rab GTPases, which created tethering interactions between different membranes through these Rab GTPases. This cumulative interaction resulted in the sequestration of membranes via aggregation (**Fig. 1b** and **Supplementary Video 2**). Transient illumination reduced the movement of endosomes, which began disaggregating and recovered their dynamics within 15 min after we withdrew the illumination (**Fig. 1c**). Aggregation of Rab5-targeted membranes was reflected by both an increase in the average size (2.1 fold after 15 min of illumination) and a decrease in the number (43% after 15 min of illumination) of fluorescent puncta (**Fig. 1d**). Moreover, the movement and average speed (1.55 μm/min versus 3.66 μm/min, respectively) of the fluorescent puncta decreased under illumination (**Fig. 1e** and **Supplementary Fig. 1d**). The Rab11-targeted membranes, which were relatively small in size, withdrew from peripheral regions and usually aggregated around the perinuclear endocytic recycling compartment (**Fig. 1f**). We also used super-resolution

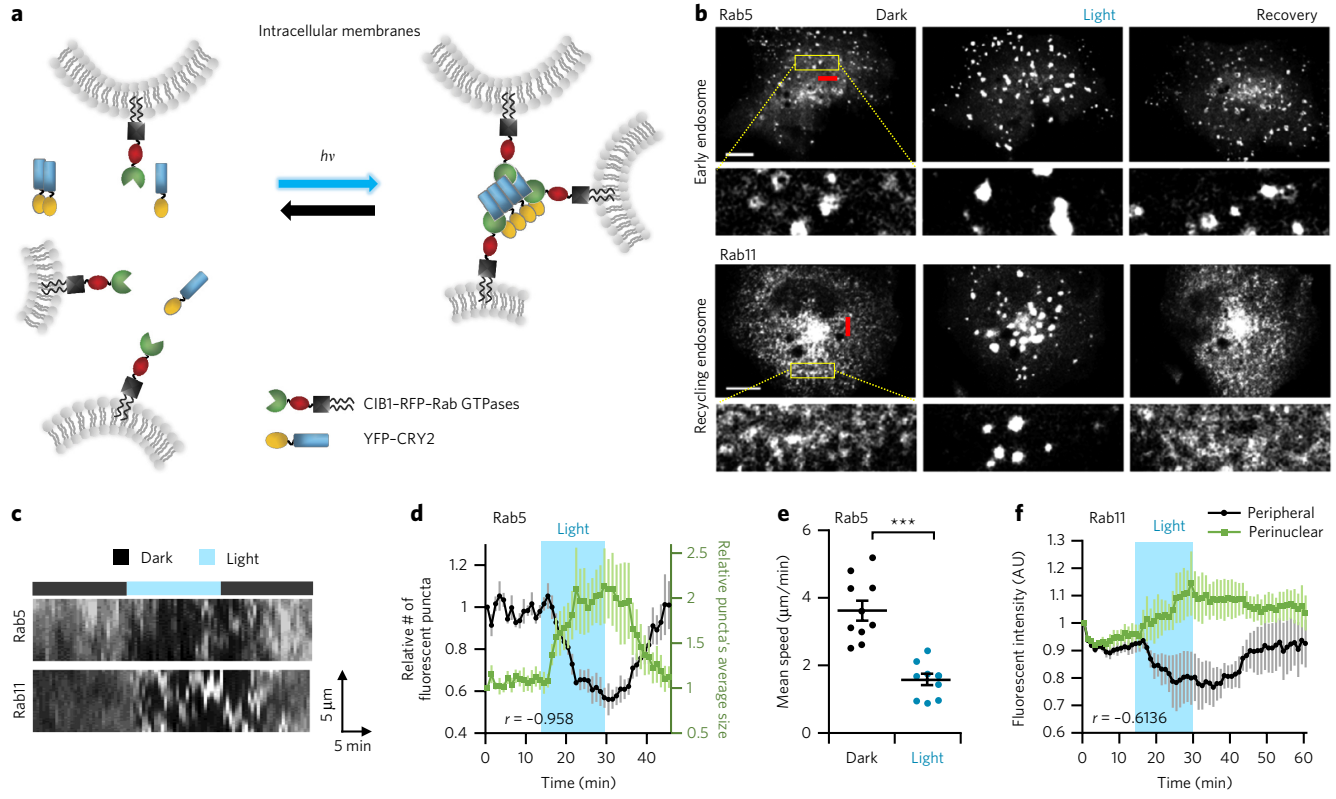

Figure 1 | Optogenetic control of intracellular membrane trafficking by light-induced aggregation of Rab GTPases. (**a**) Schematic of intracellular membrane aggregation triggered by the light-induced (*hν*) binding of CRY2- and CIB1-Rab. (**b**) Confocal images showing reversible control of early and recycling endosomes in COS-7 cell stably expressing YFP–CRY2 and transfected with sequence encoding CIB1–RFP–Rab5 or CIB1–RFP–Rab11. Yellow boxes indicate areas enlarged below. Scale bars, 10 μm. (**c**) Kymographs depicting the movements of Rab5-targeted or Rab11-targeted endosomes through the red line drawn in **b**. (**d**) Negative correlation between the relative numbers and sizes of fluorescent puncta in the CIB1–RFP–Rab5-transfected cells described in **b** (n = 4 cells, three independent experiments). (**e**) Mean speeds of endosomes in COS-7 cells stably expressing YFP–CRY2 and transfected with sequence encoding CIB1–RFP–Rab5 in the dark and during stimulation with light (15 min; n = 10 cells, three independent experiments; $^{***}P = 3.89 \times 10^{-6}$; two-tailed Student's t-test; black bars, average values). Error bars, s.e.m. (**f**) Normalized total fluorescence intensity of vesicles in perinuclear and peripheral regions of cells transfected with sequence encoding CIB1–RFP–Rab11, as in **b** (n = 4 cells, four independent experiments). AU, fluorescence intensity. r, correlation coefficient. The applied stimulating light consisted of one pulse (4.2 μW) every 30 s during 15 min.

© 2016 Nature America, Inc. All rights reserved.

structured illumination microscopy (SIM) to examine the Rab5-targeted compartment under exposure to light, and observed aggregations containing distinct vesicle-shaped structures. EEA1, which independently binds to PI3P on Rab5-targeted early endosomes, completely localized with the Rab5-targeted aggregations during stimulation with light (**Supplementary Fig. 2a**,**b**). No other membrane organelle was included in the Rab5 and Rab11-targeted aggregations, and these aggregations did not interfere with unrelated trafficking process, such as the trafficking of vesicular stomatitis virus glycoprotein (VSVG) from the Golgi to the PM (**Supplementary Fig. 2c–f**). This suggests that the aggregated Rab GTPases retained their insertions in specific intracellular membranes. The membrane aggregation triggered by IM-LARIAT therefore involves the sequestration of functional effectors that directly mediate trafficking processes.

Targeting different membranes using diverse Rab GTPases

In addition to the early endosomal and recycling compartments, we also examined the light-induced aggregation of other distinct Rab-targeted membranes, including the late endosomal compartment, secretory vesicles, the ER-to-Golgi vesicles and the Golgi-to-PM vesicles, using Rab7, Rab3a, Rab2a and Rab6a, respectively. The functions of these Rab GTPases in the indicated trafficking pathways have been previously established[19]. Upon illumination with light, Rab7- and Rab3a-targeted vesicles formed aggregates and showed decreased dynamics, which was similar to our observation with Rab5- and Rab11-targeted membranes (**Supplementary Fig. 3a–d** and **Supplementary Videos 3** and **4**). Illumination with light also caused the aggregation of membranes on the ER and Golgi when the system targeted Rab2a and Rab6a, respectively (**Supplementary Fig. 3e–h** and **Supplementary Video 5**). To confirm that the aggregation of Rab-targeted intracellular membranes was specific to the targeted membranes, we inspected other Rab-mediated trafficking pathways. We found that the aggregates of Rab5-targeted early endosomes, Rab7-targeted late compartments or Rab3a-targeted secretory vesicles did not alter the pattern or dynamics of Rab11-targeted recycling endosomes, which are localized ubiquitously throughout the cell (**Supplementary Fig. 4a–c**). We also examined the specificity of our technique by using pairs of Rab GTPases known to target the same intracellular membrane: Rab7 and Rab9 on late compartments, Rab11 and Rab25 on recycling endosomes, and Rab3a and Rab27a on secretory vesicles. We found that the oligomerization of one Rab GTPase induced the aggregation of the corresponding paired Rab GTPase (**Supplementary Fig. 4d–f**). Together, these results suggest that the aggregation of different intracellular membranes reflecting different trafficking steps could be achieved through the use of specific Rab GTPases, which retained their distinct localizations during membrane aggregation. As some Rab GTPases localize to different domains within the same intracellular compartment, aggregation of membranes targeted by a specific Rab can also result in partial aggregation of other Rab GTPases localized on the same compartment. Therefore, when using IM-LARIAT it is important to choose an appropriate target Rab GTPase.

Optogenetic control of functional trafficking processes

To confirm that light-mediated aggregation of Rab-targeted membranes triggered functional alterations in trafficking processes, we first tested the effect of Rab11-targeted aggregation on transferrin recycling (a classic function of Rab11)[19] in COS-7 cells. In the dark, most transferrin receptors were recycled after 60 min of internalization, as indicated by a notable decrease in intracellular Alexa-Fluor-conjugated transferrin (**Supplementary Fig. 5**). In illuminated cells observed for over 60 min, a substantial proportion of the transferrin receptors remained within the Rab11-targeted aggregations. After we withdrew the illumination, the Rab11-targeted endosome pattern recovered and the quantity of intracellular transferrin receptors decreased (**Fig. 2a**). To exclude the possibility that the recycling rate could have been affected by temperature variation during live-cell imaging, we examined the amount of intracellular transferrin receptors in fixed cells, and found that illumination with light reduced the transferrin recycling rate by approximately half (**Fig. 2b**). Consistent with a previous report that transferrin trafficking has little or no relationship with the late trafficking

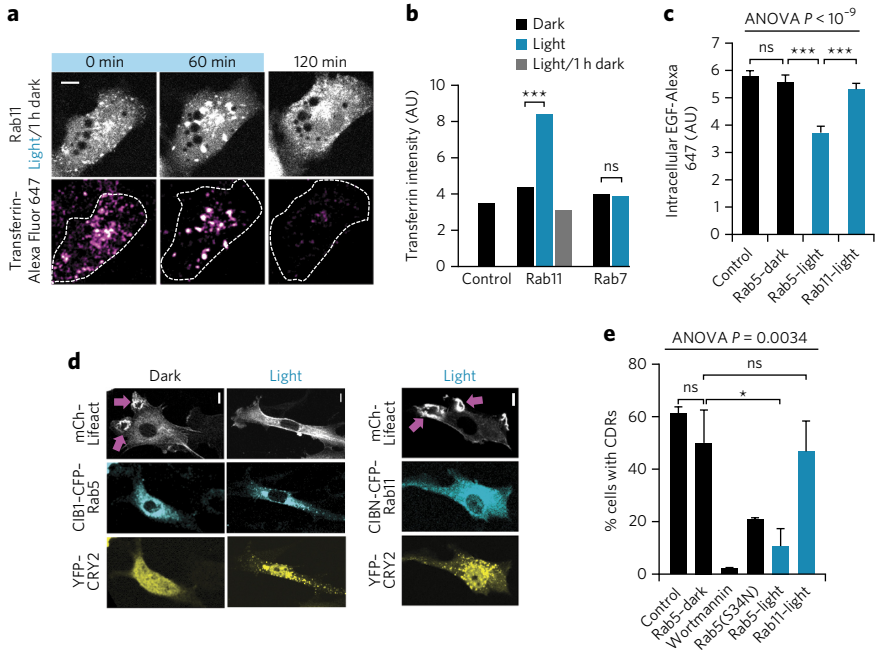

Figure 2 | Optogenetic control of specific functions mediated by Rab5-targeted and Rab11-targeted membrane. (**a**) Confocal images of COS-7 cells stably expressing YFP–CRY2 and transfected with sequence encoding CIB1–RFP–Rab11, which were loaded with transferrin–Alexa Fluor 647, followed by removal of excess ligand by washing, and subsequently tracked with stimulation by light and then without stimulation. White dotted lines depict the outlines of cells. AU, fluorescent intensity. (**b**) Transferrin intensity in COS-7 cells stably expressing YFP–CRY2 alone or transfected with sequence encoding CIB1–RFP–Rab11 or CIB1–RFP–Rab7, loaded with transferrin–Alexa Fluor 647, which were washed to remove excess ligands, and incubated in the dark or with illumination for 60 min (n = 50 cells, two independent experiments; $^{***}P = 6.1 \times 10^{-12}$; ns, $P > 0.9999$; two-tailed Student's t-test). (**c**) Intracellular intensity of EGF–Alexa Fluor 647 in COS-7 cells stably expressing YFP–CRY2 alone or co-transfected with CIB1–CFP–Rab5 or CIB1–CFP–Rab11 that were loaded with EGF–Alexa Fluor 647, incubated in the dark or illuminated conditions, with excess ligands subsequently washed off (n = 70 cells, three independent experiments; $^{***}P < 0.0001$; ns, $P > 0.9999$; two-tailed Student's t-test). (**d**) CDR formation with or without light stimulation in NIH-3T3 cells co-transfected with sequences encoding mCherry–Lifeact, YFP–CRY2 and CIB1–CFP–Rab5 or CIB1–CFP–Rab11, and treated with PDGF. (**e**) Percentage of cells that formed CDRs after PDGF treatment (n = 74 cells, three independent experiments; ns, $P > 0.9999$; $^{*}P = 0.0201$). Arrows indicate CDRs. The stimulation with consisted of one pulse of 4.2 μW every 1 min. Scale bars, 10 μm. Error bars, s.e.m.

© 2016 Nature America, Inc. All rights reserved.

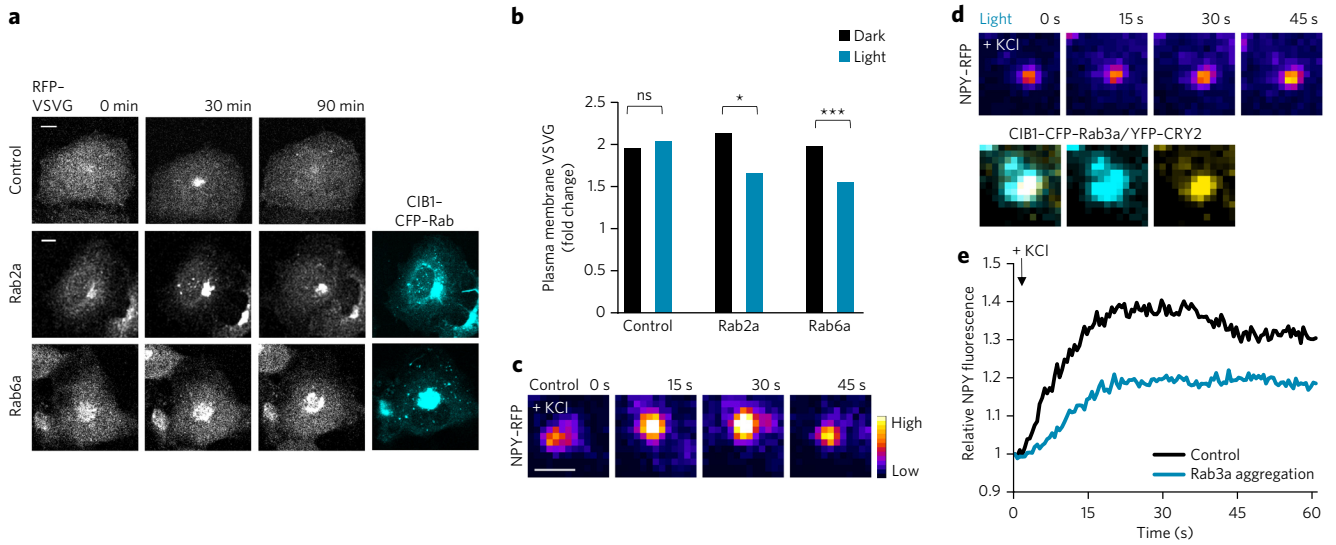

Figure 3 | Optogenetic control of specific functions mediated by diverse Rab-targeted membranes. (**a**) Time-lapse confocal microscopy at 32 °C to observe the ER-Golgi-PM transportation of VSVG vesicles in COS-7 cells stably expressing YFP–CRY2 and transfected with sequence encoding RFP–VSVG alone or with CIB1–CFP–Rab2a or CIB1–CFP–Rab6a, and subsequently incubated overnight at 40 °C to induce ER localization of VSVG. Scale bars, 10 μm. (**b**) Total internal reflection fluorescence (TIRF) microscopy of cells treated as in **a**, for detection of PM VSVG intensity before and after 90 min of incubation at 32 °C. Stimulating light was given as one pulse every 1 min (n = 60 cells, two independent experiments; ns, P = 0.65046; *P = 0.03941; ***P = 0.00017; two-tailed Student's t-test). (**c**,**d**) TIRF microscopy of Neuroscreen-1 cells transfected with sequences encoding YFP–CRY2, NPY–RFP and a CFP-null plasmid (**c**) or CIB1–CFP–Rab3a (**d**), light-induced for vesicle aggregation over 5 min (488 nm, one pulse every 500 ms) and stimulated with high KCl (60 mM). Scale bar, 1 μm. (**e**) Relative fluorescence intensities of several NPY vesicles from **c** and **d** that were stably docked during 1 min of KCl treatment and colocalized with Rab3a-targeted aggregation (n = 39 and 50 vesicles, respectively, from eight cells per group, two independent experiments).

© 2016 Nature America, Inc. All rights reserved.

pathway[23], light-mediated Rab7-targeted aggregation had no effect on transferrin recycling (**Fig. 2b**). Next, we examined the capability of our technique to disrupt another common pathway: the activation of cell surface receptors, such as the EGF receptor (EGFR). Rab5 has been well known to be involved in EGFR endocytosis[24]. In cells subjected to Rab5 aggregation but not Rab11 aggregation, the endocytosis rate of EGFR was significantly reduced, as monitored using the intracellular fluorescence intensity of EGF–Alexa Fluor 647 (**Fig. 2c** and **Supplementary Fig. 6**). Another important regulatory step in EGFR trafficking is the Rab7-mediated degradation of the receptor in the late compartment[25]. In cells subjected to light-induced Rab7 aggregation, the degradation rate of EGFR (indicated by intracellular EGF–Alexa Fluor 647) was reduced by approximately half after 2 h of stimulation (**Supplementary Fig. 7**). These results proved that by targeting different compartments and using different duration of illumination, we could control specific steps in the transportation route of cargo, such as EGFR.

A recent study suggests that intracellular membranes can function as a physical platform for the assembly of signaling complexes[2]. In cells treated with growth factors (e.g., platelet-derived growth factor; PDGF), Rab5 has been implicated in the local activation of Rac1, which in turn triggers local actin rearrangement and the formation of circular dorsal ruffles (CDRs)[20]. We therefore asked whether Rab5-targeted aggregation could abrogate the Rab5-mediated local activity of Rac1 in NIH-3T3 cells. In control cells transfected with sequence encoding mCherry-Lifeact (an F-actin biosensor) alone, 61% of the cells formed CDRs. Conversely, in cells pre-incubated with wortmannin, an inhibitor of phosphoinositide 3-kinase (PI3K; which plays a central role in Rac1 activation), CDR formation was completely disrupted. Cells transfected with the GTP-binding-deficient variant Rab5(S34N) also demonstrated reduced CDR formation (20.7% of the cells formed CDRs), confirming the importance of Rab5 in this pathway. In cells subjected to light-induced aggregation of Rab5, but not Rab11, we observed a significant decrease in number of cells with CDRs (10.7% versus 46.8%, respectively) (**Fig. 2d**,**e** and **Supplementary Video 6**). These results confirm that Rab5 and early endosome trafficking are required for signaling downstream of growth factors, and verify that Rab5-targeted aggregation abrogates the ability of Rab5-targeted endosomes to function as a signaling assembly platform.

We next validated that IM-LARIAT can be used to control not only the receptor internalization routes but also the protein secretory pathways. Rab2a and Rab6a regulate ER-Golgi-PM trafficking of secretory vesicles[19]. To test the effect of Rab2a and Rab6a aggregation, we used a VSVG variant, VSVG (tsO45), hereafter referred to as VSVG, that has been widely used to assess the transportation of secretory vesicles[26]. Newly synthesized VSVG mostly accumulated in the ER when we incubated cells at 40 °C, redistributed to the Golgi complex upon temperature shift to 32 °C, and finally transported to PM. In cells with light-induced aggregation of Rab2a or Rab6a, the transportation rate of VSVG to the PM 90 min after temperature shift was significantly delayed (1.66 fold and 1.55 fold, respectively, versus approximate twofold increase in cells incubated in the dark) (**Fig. 3a**,**b**). We also found that in neuroscreen-1 cells, light-induced Rab3a aggregation can affect the docking ability to the PM of dense-core vesicles, which was labeled using neuropeptide Y (NPY–RFP), upon stimulation with high-KCl buffer. In this case, cells with Rab3a aggregation showed reduced dynamics, ~18.8% of NPY-vesicle dynamics compared to those in cells without Rab3a aggregation (**Fig. 3c**–**e**). This result was consistent with a previous study examining the function of Rab3a in the regulation of dense-core vesicle exocytosis[27]. Collectively, our data confirmed that IM-LARIAT can specifically modulate diverse functional trafficking steps.

Rab5 and Rab11 differently regulate neuronal growth rate

Given the distinct and complex morphologies of neurons, it has proven challenging to study the intracellular vesicle trafficking that is indispensable for many neuronal functions, including cell survival, axonal growth, axonal guidance and synaptic release[28,29]. During development, vesicle trafficking in the GCs can mediate

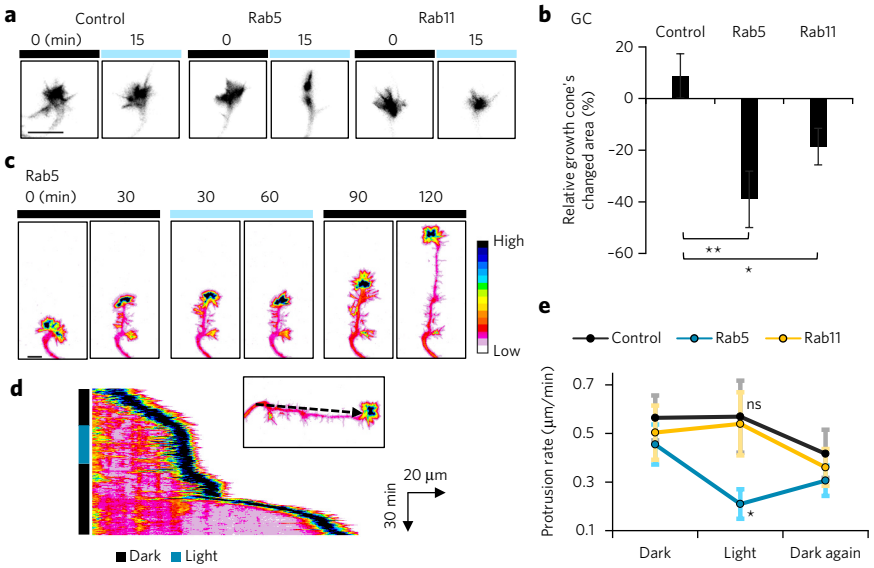

Figure 4 | Rab5-targeted and Rab11-targeted aggregations in GCs of hippocampal neurons differently interfere with protrusion and growth. (**a**) Inverted fluorescence images of mCherry–Lifeact in stable neuronal GCs subjected to local stimulation with light. Rat hippocampal neurons (DIV 3–6) were transfected with sequences encoding mCherry–Lifeact and YFP–CRY2 (control group), or with CIB1–CFP–Rab5 or CIB1–CFP–Rab11 (to target Rab5-positive or Rab11-positive membranes, respectively). (**b**) Changes in GC areas at 30 min to 60 min after local light stimulation of GCs (n = 13, 16 and13 GCs, respectively, from five to eight independent experiments; *P = 0.02683; **P = 0.002193; two-tailed Student's t-test). (**c**) Pseudocolor images of a representative neuronal GC with light-induced Rab5 aggregation that showed an average protrusion rate >0.2 μm/min during the experimental course (30 min of dark, 30 min of illumination, and 60 min of dark). Color bar shows Lifeact intensity. (**d**) Kymograph showing the movement of the GC in **c** through a line drawn along the protrusion path. (**e**) The average growth rate of fast-protruding GCs subjected to local light stimulation (n = 9 GCs from 4–8 independent experiments; *P = 0.047; ns, P = 0.88; two-tailed Student's t-test). Light stimulation was given as a 1-s pulse (4.2–7.0 μW) every 30 s or every 1 min for 30–60 min, locally at the GCs. Scale bars, 10 μm. Error bars, s.e.m.

the response to extracellular guidance cues and transportation of materials that promote the extension of neurites. The use of conventional approaches to study trafficking in neurons has often yielded unclear results regarding the functions of Rab GTPases[30] and/or induced lethality[6]. We thus first confirmed that our optogenetic tool can locally induce Rab5-targeted aggregation in the soma or GCs of neurons without interfering with Rab5-targeted endosomes in other regions (**Supplementary Fig. 8** and **Supplementary Video 7**). A previous study showed that Rab5 functions in the recycling pathway, which is necessary for the elongation of neurites[31]. Rab11 has also been implicated in regulating the trafficking of integrin to adhesive points in the GCs, a step that is also necessary for neurite growth[32]. Therefore, we asked whether the local aggregations of Rab5- or Rab11-targeted endosomes in the soma or GCs of young neurons (days *in vitro* (DIV) 3–6) would trigger a different neurite outgrowth pattern. Among the examined GCs, some were in the progression stage (with protrusion rates ≥0.2 μm/min), whereas others were in the pause stage, and were thus stable during the examined period (1–2 h)[33]. The local aggregation of Rab5- or Rab11-targeted membranes in soma did clearly alter the areas of stable GCs or the protrusion rates of progressing GCs (**Supplementary Fig. 9** and **Supplementary Video 8**). Light-induced local aggregation of Rab5 in GCs significantly decreased the areas of stable GCs (by 39.1%), most of which collapsed. Local Rab11 aggregation was associated with a smaller reduction in GC area (by 18.6%) (**Fig. 4a**,**b** and **Supplementary Video 9**). Within the fast-protruding GCs, Rab5 aggregation clearly reduced in the protrusion rate (from 0.45 μm/min to 0.21 μm/min), which was recovered upon withdrawal of illumination; in contrast, Rab11 aggregation had no significant effect (**Fig. 4c–e** and **Supplementary Video 10**). We also confirmed that the protruding phase of GCs corresponded to the recovery phase of Rab5 endosomes in the GC after illumination with light (**Supplementary Fig. 10**). Together these results suggest that, in neuronal GCs, the Rab5-mediated fast recycling pathway has an important and immediate role in accelerating the protrusion rate. Moreover, a previous study suggested that in addition to Rab11 other Rab GTPases can function as integrin carriers to the adhesive points[32]. Our results and the previous findings therefore suggest that the Rab11-targeted compartments may affect the stabilization of GCs and support dendritic growth over the long term, whereas those targeted by Rab5 may affect the immediate growth rate through the rapid production of membranes.

DISCUSSION

We developed IM-LARIAT, an optogenetic tool that can be used to control diverse intracellular membrane trafficking pathways with high specificity and reversibility. We demonstrated light-dependent control of various trafficking processes, including early-to-late endosome trafficking, recycling route, ER-Golgi-PM transport of secretory proteins and docking of dense-core secretory vesicles. Our method of inducing rapid aggregation can help reveal temporal and local roles of distinct intracellular membranes, especially in a complex system such as a neuron. As an example, we used IM-LARIAT to reveal the different spatiotemporal roles of Rab5-targeted and Rab11-targeted membranes in regulating neurite growth in hippocampal neurons. As a new optogenetic tool designed for controlling intracellular membrane trafficking, this system had several unique advantages. First, the use of diverse Rab GTPases as membrane markers allows access to specific intracellular membrane compartments. Depending on the subcellular localization and function of the target Rab GTPase, IM-LARIAT could be modified and applied for various studies on membrane trafficking. Second, the use of light as the control switch enables the control of the time and the duration of membrane aggregation. In some cases, induced membrane aggregation must be retained throughout a period of time in order to observe the effect, for example, the late trafficking stage of EGFR. This advantage of IM-LARIAT is particularly useful in the studies of membrane trafficking during development of embryos *in vivo*, especially the processes that mediated by the vital Rab GTPases.

A similar strategy has been used previously to rapidly sequester intracellular membrane, called "knock sideways"[34]; that technique rerouted membrane adaptors to mitochrondria using rapamycin-induced heterodimerization. Our optogenetic approach adds to this body of work and offers a useful tool for dissecting the details of local and immediate functions of membranes, especially in specific tissue regions or neuronal compartments. More recently, several groups demonstrated that the recruitment of motor proteins to membrane organelles can induce repositioning of those organelles[35,36]. The researchers controlled the direction of organelle transportation to gain insights into the local distribution and functions. As an alternate approach, IM-LARIAT provides a new method to spatiotemporally

© 2016 Nature America, Inc. All rights reserved.

inhibit membrane functions without inducing the recruitment of motors to membranes. Here we used diverse Rab GTPases to target a wider range of membrane types, including ER and Golgi, which cannot be easily modulated by the recruitment of motors. The triggered aggregation did not cause major changes in the localization of membrane organelles, and thus allowed for a quicker recovery with fewer side effects, compared to the uncertain recovery process seen after the motor-driven withdrawal of membranes. We believe our technique will be important for the study of polarized trafficking processes in neurons, such as efforts to examine the immediate roles of different membrane compartments during neurite growth and extension, and the roles of ER and Golgi outposts in the local trafficking of neurons[28,37].

Although our expression of wild-type Rab GTPase is a standard and acceptable technique for studying the function of a protein in cell culture, the potential effect of this expression should be carefully considered in studies using neurons or higher model systems. In the future, we plan to combine our tool with genome editing, which we will use to specifically insert sequence encoding CIB1 into the genome, enabling us to optogenetically control the intracellular membrane using endogenous proteins.

Received 10 December 2015; accepted 7 March 2016; published online 11 April 2016

METHODS

Methods and any associated references are available in the online version of the paper.

References

1. Sadowski, L., Pilecka, I. & Miaczynska, M. Signaling from endosomes: location makes a difference. *Exp. Cell Res.* **315**, 1601–1609 (2009).
2. Pálfy, M., Reményi, A. & Korcsmáros, T. Endosomal crosstalk: meeting points for signaling pathways. *Trends Cell Biol.* **22**, 447–456 (2012).
3. Théry, C., Ostrowski, M. & Segura, E. Membrane vesicles as conveyors of immune responses. *Nat. Rev. Immunol.* **9**, 581–593 (2009).
4. Goldenring, J.R. A central role for vesicle trafficking in epithelial neoplasia: intracellular highways to carcinogenesis. *Nat. Rev. Cancer* **13**, 813–820 (2013).
5. Millecamps, S. & Julien, J.-P. Axonal transport deficits and neurodegenerative diseases. *Nat. Rev. Neurosci.* **14**, 161–176 (2013).
6. Zhang, J. *et al.* Thirty-one flavors of *Drosophila* rab proteins. *Genetics* **176**, 1307–1322 (2007).
7. Gillespie, E.J. *et al.* Selective inhibitor of endosomal trafficking pathways exploited by multiple toxins and viruses. *Proc. Natl. Acad. Sci. USA* **110**, E4904–E4912. http://dx.doi.org/10.1073/pnas.1302334110 (2013).
8. Fili, N., Calleja, V., Woscholski, R., Parker, P.J. & Larijani, B. Compartmental signal modulation: Endosomal phosphatidylinositol 3-phosphate controls endosome morphology and selective cargo sorting. *Proc. Natl. Acad. Sci. USA* **103**, 15473–15478 (2006).
9. Kennedy, M.J. *et al.* Rapid blue-light-mediated induction of protein interactions in living cells. *Nat. Methods* **7**, 973–975 (2010).
10. Bugaj, L.J., Choksi, A.T., Mesuda, C.K., Kane, R.S. & Schaffer, D.V. Optogenetic protein clustering and signaling activation in mammalian cells. *Nat. Methods* **10**, 249–252 (2013).
11. Konermann, S. *et al.* Optical control of mammalian endogenous transcription and epigenetic states. *Nature* **500**, 472–476 (2013).
12. Lee, S. *et al.* Reversible protein inactivation by optogenetic trapping in cells. *Nat. Methods* **11**, 633–636 (2014).
13. Chang, K.Y. *et al.* Light-inducible receptor tyrosine kinases that regulate neurotrophin signalling. *Nat. Commun.* **5**, 4057 (2014).
14. Kim, N. *et al.* Spatiotemporal control of fibroblast growth factor receptor signals by blue light. *Chem. Biol.* **21**, 903–912 (2014).
15. Kyung, T. *et al.* Optogenetic control of endogenous $Ca^{(2+)}$ channels *in vivo*. *Nat. Biotechnol.* **33**, 1092–1096 (2015).
16. Chen, D., Gibson, E.S. & Kennedy, M.J. A light-triggered protein secretion system. *J. Cell Biol.* **201**, 631–640 (2013).
17. Stenmark, H. Rab GTPases as coordinators of vesicle traffic. *Nat. Rev. Mol. Cell Biol.* **10**, 513–525 (2009).
18. Pfeffer, S.R. Rab GTPase regulation of membrane identity. *Curr. Opin. Cell Biol.* **25**, 414–419 (2013).
19. Hutagalung, A.H. & Novick, P.J. Role of Rab GTPases in membrane traffic and cell physiology. *Physiol. Rev.* **91**, 119–149 (2011).
20. Palamidessi, A. *et al.* Endocytic trafficking of Rac is required for the spatial restriction of signaling in cell migration. *Cell* **134**, 135–147 (2008).
21. Dou, Z. *et al.* Class IA PI3K p110β subunit promotes autophagy through Rab5 small GTPase in response to growth factor limitation. *Mol. Cell* **50**, 29–42 (2013).
22. Rosenfeldt, G., Viana, R.M., Mootz, H.D., von Arnim, A.G. & Batschauer, A. Chemically induced and light-independent cryptochrome photoreceptor activation. *Mol. Plant* **1**, 4–14 (2008).
23. Killisch, I. *et al.* Characterization of early and late endocytic compartments of the transferrin cycle. Transferrin receptor antibody blocks erythroid differentiation by trapping the receptor in the early endosome. *J. Cell Sci.* **103**, 211–232 (1992).
24. Barbieri, M.A., Fernandez-Pol, S., Hunker, C., Horazdovsky, B.H. & Stahl, P.D. Role of rab5 in EGF receptor-mediated signal transduction. *Eur. J. Cell Biol.* **83**, 305–314 (2004).
25. Ceresa, B.P. & Bahr, S.J. rab7 activity affects epidermal growth factor:epidermal growth factor receptor degradation by regulating endocytic trafficking from the late endosome. *J. Biol. Chem.* **281**, 1099–1106 (2006).
26. Presley, J.F. *et al.* ER-to-Golgi transport visualized in living cells. *Nature* **389**, 81–85 (1997).
27. Tsuboi, T. & Fukuda, M. Rab3A and Rab27A cooperatively regulate the docking step of dense-core vesicle exocytosis in PC12 cells. *J. Cell Sci.* **119**, 2196–2203 (2006).
28. Sann, S., Wang, Z., Brown, H. & Jin, Y. Roles of endosomal trafficking in neurite outgrowth and guidance. *Trends Cell Biol.* **19**, 317–324 (2009).
29. Kalil, K., Li, L. & Hutchins, B.I. Signaling mechanisms in cortical axon growth, guidance, and branching. *Front. Neuroanat.* **5**, 62 (2011).
30. Villarroel-Campos, D., Gastaldi, L., Conde, C., Caceres, A. & Gonzalez-Billault, C. Rab-mediated trafficking role in neurite formation. *J. Neurochem.* **129**, 240–248 (2014).
31. Falk, J., Konopacki, F.A., Zivraj, K.H. & Holt, C.E. Rab5 and Rab4 regulate axon elongation in the *Xenopus* visual system. *J. Neurosci.* **34**, 373–391 (2014).
32. Eva, R. *et al.* Rab11 and its effector Rab coupling protein contribute to the trafficking of beta 1 integrins during axon growth in adult dorsal root ganglion neurons and PC12 cells. *J. Neurosci.* **30**, 11654–11669 (2010).
33. Lowery, L.A. & Van Vactor, D. The trip of the tip: understanding the growth cone machinery. *Nat. Rev. Mol. Cell Biol.* **10**, 332–343 (2009).
34. Robinson, M.S., Sahlender, D.A. & Foster, S.D. Rapid inactivation of proteins by rapamycin-induced rerouting to mitochondria. *Dev. Cell* **18**, 324–331 (2010).
35. van Bergeijk, P., Adrian, M., Hoogenraad, C.C. & Kapitein, L.C. Optogenetic control of organelle transport and positioning. *Nature* **518**, 111–114 (2015).
36. Duan, L. *et al.* Optogenetic control of molecular motors and organelle distributions in cells. *Chem. Biol.* **22**, 671–682 (2015).
37. Ramírez, O.A. & Couve, A. The endoplasmic reticulum and protein trafficking in dendrites and axons. *Trends Cell Biol.* **21**, 219–227 (2011).

Acknowledgments

We thank N. Kim, H. Lee and M. Lee for helpful discussions, and D. Woo, H. Jung and S. Kim for technical assistance in neuron culture. This work was supported by the Institute for Basic Science (no. IBS-R001-G1); KAIST Institute for the BioCentury, Republic of Korea; and the Intelligent Synthetic Biology Center of the Global Frontier Project (2011-0031955) funded by the Ministry of Science, ICT and Future Planning, Republic of Korea.

Author contributions

M.K.N. and W.D.H. conceived the idea. M.K.N. and C.Y.K. designed and performed the experiments. M.K.N., C.Y.K. and J.M.K. analyzed the data. M.K.N., C.Y.K., J.M.K., B.O.P., S.L., H.P. and W.D.H. discussed the data. M.K.N. and W.D.H. wrote the paper.

Competing financial interests

The authors declare no competing financial interests.

Additional information

Any supplementary information, chemical compound information and source data are available in the online version of the paper. Reprints and permissions information is available online at http://www.nature.com/reprints/index.html. Correspondence and requests for materials should be addressed to W.D.H.

© 2016 Nature America, Inc. All rights reserved.

ONLINE METHODS

Plasmid construction. YFP–CRY2 sequence construction with mammalian codon optimization has been described in previous study[12]. To generate sequence encoding CIB1–RFP–Rab small GTPase constructs, sequence encoding CIB1 amino acids 1–170 with nuclear localization signal deleted[9] and FusionRed sequences flanked by NheI-AgeI and AgeI-BsrGI respectively, were PCR-amplified and inserted to replace *EGFP* sequence in EGFP–C1 plasmid (Clontech). *CIB1–FusionRed* combined sequence was then cut at NheI and BrsGI sites and inserted to replace *CFP* sequence in CFP–Rab plasmids obtained from small GTPase library[38]. RFP–Rab plasmids were constructed by inserting *FusionRed* sequence in the *CFP* sequence position of the CFP–Rab plasmids excised with AgeI and BsrGI sites. Similarly, CIB1–CFP–Rab plasmids were made by replacing *FusionRed* with *mCerulean* sequence flanked by AgeI and BsrGI sites. To generate CRY2–RFP–Rab5B plasmid, sequence encoding CRY2 flanked with NheI and AgeI sites[12] and *FusionRed* sequence flanked by AgeI and BsrGI sites were excised and inserted to replace *CFP* sequence in CFP–Rab5 plasmid. mCherry–Lifeact and iRFP670–Lifeact plasmid was generated based on GFP–Lifeact, from which *GFP* sequence was replaced with *mCherry* sequence or *iRFP670* sequence at NheI and BsrGI sites. The plasmids encoding YFP–Rab5B (S34N), CFP–Rac1, mCherry–PH_{AKT} and RFP–$EEA1^{FYVE}$ were obtained from previous study[38–40]. VSVG–RFP plasmid was generated by replacing *EGFP* in VSVG–EGFP plasmid (gift from J. Lippincott-Schwartz; Addgene plasmid 11912) with *FusionRed* flanked with BamHI and BsrGI sites. NPY–RFP plasmid was generated by replacing *Venus* in NPY–Venus plasmid (from A. Miyawaki, Riken Brain Science Institute) with RFP sequence flanked by AgeI and BsrGI sites.

Cell culture and transfection. COS-7 cells (ATCC) were maintained in Dulbecco's modified Eagle's medium (DMEM, Gibco, Life Technologies) supplemented with 10% FBS (Invitrogen) at 37 °C and 10% CO_2. NIH-3T3 cells (ATCC) were maintained in DMEM supplemented with 10% calf serum (Bovine serum, Gibco) at 37 °C and 10% CO_2. HeLa cells (ATCC) were maintained in Dulbecco's modified Eagle's medium (DMEM, Gibco, Life Technologies) supplemented with 10% FBS (Invitrogen) at 37 °C and 10% CO_2. Neuroscreen-1 cells (subclone of PC-12 cells; Cellomics) were provided by T. Meyer (Stanford University) and maintained in F-12K medium (Cellgro, 10-025-CV) supplemented with 15% horse serum (Gibco, 16050-122) and 5% FBS at 37 °C and 5% CO_2. These cell lines were confirmed to be free from mycoplasma before use by using e-Myco Mycoplasma PCR detection kit (ver. 2.0, iNtRON). COS-7 cells were plated on a μ-Plate 96 Well ibiTreat (ibidi, 89626) and transfected using Lipofectamine LTX (Invitrogen) according to the manufacturer's instructions. In experiments using TIRF microscopy, COS-7 cells were transfected using a Microporator (Neon Transfection System, Invitrogen), with the modified condition (950 V, 10 ms, 3 pulses) and plated on 8-well Lab-Tek II Chambered Coverglass (Thermo Scientific, 155409) or 96-well chamber slide (MatriCal, MGB096-1-2-LG-1). NIH3T3 cells were transfected using a microporator, with modified conditions (1,410 V, 10 ms, 3 pulses*)* and plated on a μ-Plate 96 Well ibiTreat precoated with 100 μg/ml poly(D-lysine) (Sigma-Aldrich, P6407). HeLa cells were plated on six-well plate (Corning, Sigma-Aldrich, CLS3516) and transfected using Lipofectamine RNAimax (Invitrogen, 13778-075) according to the manufacturer's instructions.

Preparation and transfection of hippocampal neurons. All hippocampal neurons were prepared from embryos obtained from E18 pregnant Sprague-Dawley female rats. All the experimental steps were strictly followed the regulations of the Animal Ethic Committee at the Korea Advanced Institute of Science and Technology (KAIST). The detailed procedure was described before[13]. In brief, neurons dissected and triturated from hippocampi were plated on pre-equilibrated μ-Plate 96 Well ibiTreat coated with 0.1 mg/ml poly(L-lysine) (Sigma), together with plating medium and incubated at 37 °C and 5% CO_2. The plating and maintaining medium consisted of Neurobasal medium (Gibco), 2% glutamax (Gibco), 2% penicillin-streptomycin (Gibco) and 2% FBS or 2% B-27 (Gibco), respectively. Neuron transfection was performed using Lipofectamine LTX, with DNA amount, plus reagent and Lipofectamine used as 1:1:1 ratio, diluted in fresh maintaining medium, followed by a change to old medium after 30–60 min.

Live-cell imaging. All transfected cells and neurons were covered with aluminum foil to be protected from light before imaging. Cells were imaged within 15–24 h after transfection. NIH-3T3 cells were additionally starved in DMEM with 1% calf serum for up to 6 h before imaging. In experiments using COS-7 and NIH-3T3 cells, the medium was replaced with OPTI-MEM I (Invitrogen) shortly before imaging. Live-cell imaging was performed using a Nikon A1R confocal microscope mounted onto a Nikon Eclipse Ti body and equipped with CFI Plan Apochromat VC objectives (60×, numerical aperture (NA) 1.4, oil, or 40×, NA 0.95, air), and Nikon superresolution structured illumination (SIM) microscope with CFI SR Apochromat objective (100×, NA 1.49, oil, 3D-SIM mode) (**Supplementary Fig. 2**). CFP (mCerulean), GFP, mCitrine, mCherry (FusionRed, Alexa Fluor 594) and iRFP670 (Alexa Fluor 640) were taken using 547-, 488-, 514-, 561- and 640-nm lasers, respectively. In some experiments 488-nm laser was also used to image mCitrine. Light stimulation was performed with 488-nm laser or 459-nm laser in some cases. In transferrin internalization assay, we used a customized LED array to light-stimulate cells seeded in 96-well plates. The LEDs emitted an equal intensity of blue light (488 nm) onto the bottom of the plate (5.5 μW/cm^2), and were used as 10-s irradiations per minute. The irradiating duration and intervals were controlled using built-in software. To perform local photoactivation, we used a 488-nm laser emitted through a Galvano scanner with a hybrid confocal scan head containing a high-speed hyper selector (Nikon) that can excite the defined volume (for example, the tip of growth cone, soma area in single neuron). The intensity of the stimulation light was measured on the focus plane with an optical power meter (catalog no. 8230E, ADCMT). The laser intensity used in all experiments was 2.1–4.2 μW, which corresponds to 4.7–10 mW/cm^2.

To visualize plasma membrane or vesicles near plasma membrane (VSVG trafficking assay and Rab3-related assay), we used a Nikon Ti-E total internal reflection fluorescence (TIRF) microscope equipped with a CFI Apochromat TIRF 60× objective. A double laser for GFP (488 nm) and RFP (561 nm) (CVI-Melles Griot) were used to produce stimulation light. Emission filter fluorescein isothiocyanate (FITC HYQ) and tetramethylrhodamine (TRITC) (96320, Nikon) were used for GFP and RFP, respectively; and an electron-multiplying charge-coupled device (EMCCD) camera (C9100-02, Hamamatsu Photonics) was used as a detector.

Reagents and antibodies. Alexa-Fluor-647-conjugated transferrin was purchased from Invitrogen–Molecular Probes (T23366) and used at a concentration of 30 μg/ml. EGF conjugated with Alexa Fluor 647 was purchased from Invitrogen–Molecular Probes (E35351) and used at the concentration of 1 μg/ml. PDGF-BB from Peprotech (100-14B) was used at 10 nM concentration. EEA1 antibody was purchased from Cell Signaling Technology (C45B10, 1:100 dilution). Rab5B and GAPDH antibody was purchase from Santa Cruz Biotechnology (sc-598, sc-25778). Goat anti-rabbit IgG (H+L) secondary antibody, with Alexa Fluor 647 conjugate was purchased from Thermo Fisher Scientific Inc. (A-21245). Goat anti-rabbit IR dye 600CW was purchased from LI-COR (626-68071).

siRNA. Synthetic CDS Rab5b siRNA was purchased from Santa Cruz Biotechnology (sc-36346). To generate Rab5b UTR siRNA, gene-specific primers were automatically designed with an in-house primer program and were used to generate ~560 bp cDNA fragments immediately downstream of the stop codon of mRNA by PCR. An additional set of nested primers was designed to add T7 promoters at both ends of the final cDNA fragment. Nested PCR products were subjected to *in vitro* transcription (T7 MEGA script kit, Ambion), *in vitro* dicing (Purified Giardia Dicer), and purification to produce siRNA as described previously[41,42]. Gene specific primers were: forward, agcagcaaacaagtatggagc and reverse, cctccacaaggccaaatcatg. Nested primers were: forward, gcgtaatacgactcactataggataacctccatccctaccc and reverse, gcgtaatacgactcactataggcaaatatgagaaactccaacc.

Transferrin recycling assay and EGFR trafficking assay. Alexa Fluor 647 conjugated with transferrin was diluted in full DMEM (30 μg/ml), added to cells in 96-well plates, and incubated at 37 °C for 15–20 min to allow transferrin receptor internalization. After that, cells were cooled to 4 °C to halt endocytosis, washed with ice-cold PBS once to remove unbound ligands, and stripped

© 2016 Nature America, Inc. All rights reserved.

of surface-bound ligands for 1 min with ice-cold PBS at low pH once, then washed twice with cold OPTI-MEM I. Warmed OPTI-MEM I was then added for live-cell imaging. For data shown in **Figure 2c**, cells were then incubated at 37 °C with different conditions and durations, then fixed in 4% paraformaldehyde and washed several times with PBS.

To quantify the intracellular transferrin, cell images were acquired at the same laser power, same depth value. Acquired images were then normalized using the background by dividing by the intensity of 1 μm^2 area from the blank region without cell.

EGF–Alexa Fluor 647 was diluted in OPTI-MEM I (1 μg/ml), added to cells in 96-well plates and incubated at 37 °C for 10 min to induce EGF receptor internalization. After that, cells were cooled to 4 °C to halt endocytosis, washed with ice-cold PBS once to remove unbound ligands, stripped surface-bound ligands for 1 min with ice-cold PBS at low pH once, then washed twice with cold OPTI-MEM I. Warm OPTI-MEM I was then added for live-cell imaging. In EGFR-degradation assay, cells were then incubated at 37 °C for 2 h, fixed in 4% paraformaldehyde and washed several times with PBS before quantified for intracellular EGF–Alexa Fluor 647.

Western blot analysis. Whole-cell lysates were prepared using PRO-PREP solution (17081; iNtRON Biotechnology). 20 μg of total protein was loaded on a NuPAGE Novex 8% Bis-Tris gel (Invitrogen) and then transferred to a nitrocellulose membrane using an iBlot Transfer Stack and iBlot Gel Transfer Device (Invitrogen) according to the manufacturer's instructions. The membrane was then incubated with primary Rab5b antibody (1:200) overnight at 4 °C, followed by GAPDH antibody incubation (1:500) and secondary antibody (goat anti-rabbit IR Dye 600CW, 1:2,000). These blots were scanned by Odyssey CLx Infrared Imaging system (LI-COR).

Image processing and analysis. Processing of all images was done using NIS-elements and Fiji 1.49u software. Some of the time-lapse images were shift-corrected and bleach-corrected using StackReg and Bleach Correction plugins, respectively, in Fiji. Vesicle's movement, average size and mean speed were analyzed using TrackMate plugin in Fiji. To quantify the number and sizes of fluorescent puncta, we used the manual Fiji's Threshold and Analyse Particles functions. In some cases, images of Lifeact were changed to inverted 16-colored images. Kymographs were created using Kymograph function in Fiji.

Neuronal growth cone imaging and analysis. *Growth cone area measurement.* Only growth cones with protrusion rate less than 0.2 μm/min over the experimental course were analyzed. The area counted for each growth cone was the average area measured during the last 1 min (3 frames) of each phase (dark, light or dark again).

Growth cone protrusion rate measurement. Only growth cones with protrusion rate more than 0.2 μm/min over the experimental course were analyzed. Measurement was performed according to the differences in position of growth cone's stem (where the fan shape of lamellipodia starts) using NIS-elements.

Statistical analysis. The difference between two groups was analyzed using Student's two-tailed *t*-test. Multiple comparison in a group was performed using one-way analysis of variance (ANOVA), and pairwise comparison in a group was corrected using the Bonferroni method. Statistical analysis was performed using Analysis ToolPak-VBA in Excel and GraphPad's Prism 6.

38. Heo, W.D. & Meyer, T. Switch-of-function mutants based on morphology classification of Ras superfamily small GTPases. *Cell* **113**, 315–328 (2003).
39. Yang, H.W. *et al.* Cooperative activation of PI3K by Ras and Rho family small GTPases. *Mol. Cell* **47**, 281–290 (2012).
40. Gil, J.E. *et al.* Phosphoinositides differentially regulate protrudin localization through the FYVE domain. *J. Biol. Chem.* **287**, 41268–41276 (2012).
41. Matsui, T., Itoh, T. & Fukuda, M. Small GTPase Rab12 regulates constitutive degradation of transferrin receptor. *Traffic* **12**, 1432–1443 (2011).
42. Park, B.O., Ahrends, R. & Teruel, M.N. Consecutive positive feedback loops create a bistable switch that controls preadipocyte-to-adipocyte conversion. *Cell Rep.* **2**, 976–990 (2012).

© 2016 Nature America, Inc. All rights reserved.

doi:10.1038/nchembio.2064